

Nonlinear magneto-optical Kerr spectra of thin ferromagnetic iron films calculated with *ab initio* theory

U. Pustogowa, W. Hübner, and K. H. Bennemann

Institute for Theoretical Physics, Freie Universität Berlin, Arnimallee 14, D - 14195 Berlin, Germany

T. Kraft

Fritz-Haber-Institut der Max-Planck-Gesellschaft, Faradayweg 4-6, D - 14195 Berlin, Germany

Abstract

Using a spin-polarized full-potential linear muffin-tin orbital method we present calculations of the nonlinear magneto-optical Kerr effect for thin *bcc* Fe films within a slab geometry. Film layer dependent contributions to the Kerr spectrum are determined. Thus, we calculate the magneto-optical Kerr spectra for the linear and nonlinear case. Our results show clearly that the Kerr spectra of thin films are characteristicly different from those at surfaces of bulk materials. In the case of linear Kerr spectra of Au/Fe(*bcc*)/Au(001) films our theoretical results are in good agreement with observed frequency- and thickness-dependent spectra.

75.30.Pd,78.20.Ls,73.20.At,75.50.Bb

I. INTRODUCTION

The nonlinear magneto-optical Kerr effect (NOLIMOKE) has been proven to be a sensitive probe for the electronic, magnetic, and symmetry properties of ferromagnetic surfaces and to yield new results. For example, it was shown theoretically [1] and experimentally [2–5], that the nonlinear Kerr rotation angle is significantly enhanced compared to the linear Kerr angle and furthermore that the Kerr spectra exhibit characteristic features of the bandstructure [6]. Thus, one expects that NOLIMOKE will be also a successful tool to study magnetic multilayers with contributions of every interface within the light penetration depth. Actually, experiments at a Co/Au multilayer system [7] show the dependence of the reflected second-harmonic intensity on the number of interfaces. In view of the surface sensitivity of NOLIMOKE it is necessary for comparison of theory with experiments to perform electronic calculations for NOLIMOKE in thin films. We show that it will not be sufficient to simulate films by simply scaling calculations of bulk surfaces. Actually, linear surface MOKE experiments on Au/Fe(*bcc*)/Au(001) observe new structures in the frequency-dependent Kerr spectrum for thin Fe films [8]. Possibly, even quantum-well states are reflected in recent experiments on this system [9].

In view of this we performed the first *ab initio* calculations of magneto-optical Kerr spectra for *bcc* Fe films with varying thickness. The film bandstructure is calculated using the spin-polarized full-potential linear muffin-tin orbital method (FP-LMTO). For comparison with the experiment we performed all calculations for nonlinear and linear Kerr spectra. Note, in our calculations we use \mathbf{k} -independent transition matrix elements and thus we have to implement the surface sensitivity. For this we use two models: (i) We take the first layer as an effective response volume. (ii) The surface response is calculated directly by projecting the wave functions to the top film layer. Hence we assume that the nonlinear response results only from the surface layer. The nonlinear response senses only the electronic structure of the first two top film layers, whereas in the case of linear response the electronic structure of the whole film is involved. This is found to be in agreement with experiments [10–13].

To simulate structural film effects we perform calculations for different film lattice constants.

In order to check the validity of using and scaling bulk parameters for film calcula-

tions, we compare the monolayer and the bulk *ab initio* calculated spectra with results of semi-empirical tight-binding calculations using scaled parameters to simulate the reduced dimension. The semi-empirical monolayer spectrum is calculated firstly on the basis of a three-dimensional bandstructure with bulk parameters scaled with the square root of the coordination number and secondly using a two-dimensional bandstructure. We find that scaled bulk parameters are not sufficient to characterize film spectra properly.

For the two-dimensional semi-empirical calculations, spin-orbit coupling is treated using two different approximations: First, we calculate spin-orbit coupling non-perturbatively in the Hamiltonian. Secondly, we employ first-order perturbation theory. Thus, we are able to prove the linear dependence of the nonlinear Kerr effect on spin-orbit coupling.

In Section II we outline our electronic theory for the film calculations, in Section III we present results and these are discussed in Section IV. Summarizing, our results show that: (i) Nonlinear Kerr spectra reflect the film structure more sensitively than linear ones. (ii) Nonlinear Kerr spectra reveal special features of films and monolayers which are different from those of bulk surfaces. Our results indicate a magnetic moment enhancement at surfaces and interfaces and in thin films.

II. THEORY

The nonlinear magneto-optical surface susceptibility $\chi^{(2)}(2q_{\parallel}, 2\omega, \mathbf{M})$ was derived within an microscopic and electronic theory by Hübner *et al.* [14,15]. The calculations of the nonlinear magneto-optical Kerr spectra of Ni and Fe surfaces of bulk crystals [6] use the following expression

$$\begin{aligned} \chi_{xzz}^{(2)}(2q_{\parallel}, 2\omega, \mathbf{M}) &= \frac{e^3 C \lambda_{s.o.}}{\Omega \hbar \omega} \\ &\times \sum_{\sigma} \sum_{\mathbf{k}, l, l'} \left\{ \langle \mathbf{k} + 2\mathbf{q}_{\parallel}, l'' \sigma | z | \mathbf{k} l \sigma \rangle \langle \mathbf{k} l \sigma | z | \mathbf{k} + \mathbf{q}_{\parallel}, l' \sigma \rangle \langle \mathbf{k} + \mathbf{q}_{\parallel}, l' \sigma | z | \mathbf{k} + 2\mathbf{q}_{\parallel}, l'' \sigma \rangle \right. \\ &\times \left. \frac{\frac{f(E_{\mathbf{k}+2\mathbf{q}_{\parallel}, l'' \sigma}) - f(E_{\mathbf{k}+\mathbf{q}_{\parallel}, l' \sigma})}{E_{\mathbf{k}+2\mathbf{q}_{\parallel}, l'' \sigma} - E_{\mathbf{k}+\mathbf{q}_{\parallel}, l' \sigma} - \hbar\omega + i\hbar\alpha_1} - \frac{f(E_{\mathbf{k}+\mathbf{q}_{\parallel}, l' \sigma}) - f(E_{\mathbf{k}l \sigma})}{E_{\mathbf{k}+\mathbf{q}_{\parallel}, l' \sigma} - E_{\mathbf{k}l \sigma} - \hbar\omega + i\hbar\alpha_1}}{E_{\mathbf{k}+2\mathbf{q}_{\parallel}, l'' \sigma} - E_{\mathbf{k}l \sigma} - 2\hbar\omega + i2\hbar\alpha_1}} \right\}, \end{aligned} \quad (1)$$

where $\lambda_{s.o.}$ is the spin-orbit coupling constant, $E_{\mathbf{k}l \sigma}$ are the electronic energy levels resulting from the bandstructure calculations, and the factor C determines the surface treatment as

discussed below. The other symbols are the same as in previous studies (e.g. [6]). Here, we present the susceptibility tensor element χ_{xzz} as a typical odd element in the longitudinal Kerr geometry (M parallel to the y axis, p -polarized incident electric field). Other magnetic (odd) and nonmagnetic (even) tensor elements can be written similarly. This formula applies also to films. Thus, the bandstructure $E_{\mathbf{k}l\sigma}$ and the transition matrix elements are calculated for films. For the film calculation we use wave functions in the transition matrix elements which depend on the position of the appropriate atom in the film. This is necessary for determining layer-dependent contributions.

The surface sensitivity of the nonlinear Kerr effect and thus $\chi^{(2)}$ is controlled by the breakdown of inversion symmetry and is essentially determined by the three transition matrix elements. These sense the necessary breakdown of inversion symmetry. Previous calculations of nonlinear and linear Kerr spectra of Ni have shown that the position of the main structures in $\chi^{(2)}$ and the peak height ratio of $\chi^{(2)}$ do not depend on the k dependence of the transition matrix elements [15]. Mainly, the energy eigenvalues define the spectral structure. This was checked by comparison of MOKE calculations and experimental obtained spectra. Thus, we use in our calculations constant transition matrix elements and simulate the surface sensitivity by an additional factor C : (i) $C = q_{\parallel}a$ in the case of the surface of bulk material, where q_{\parallel} is the component of the photon wave vector parallel to the surface and a is the lattice constant. This factor gives the ratio of the response depth a to the excitation depth in the crystal ($\approx 1/q_{\parallel}$). (ii) In the case of films we use (a) $C = 1/n^3$, with n atomic layers in the film and alternatively (b) $C = W_{\mathbf{k}+2\mathbf{q}_{\parallel},l''\sigma}W_{\mathbf{k}+\mathbf{q}_{\parallel},l'\sigma}W_{\mathbf{k}l\sigma}$, where W_{α} denotes the weight of the density of state $|\mathbf{k}l\sigma\rangle$ in the Wigner-Seitz cell of the first monolayer. The expression (a) follows from taking into account only the surface monolayer response whereby a film averaged electronic structure is used. The factor $1/n^3$ results from the fact that all three states involved in the optical transition must be localized in the first layer. (b) The factor $C = W_{\mathbf{k}+2\mathbf{q}_{\parallel},l''\sigma}W_{\mathbf{k}+\mathbf{q}_{\parallel},l'\sigma}W_{\mathbf{k}l\sigma}$ results from the projection of the six wavefunctions in the three matrix elements to atoms in the first layer. Obviously this will be the better approximation.

The most important input for the calculation of the nonlinear susceptibility is the electronic bandstructure. For thin Fe films we calculate the bandstructure within the full-

potential linear muffin-tin orbital method (FP-LMTO) developed by M. Methfessel *et al.* [16] in the spin-polarized version by M. van Schilfgaarde, adapted by one of the present authors (T. K.) for *fcc* and *bcc* Fe films on several substrates [17]. Thus, we combine the advantages of a parameter-free density-functional method with the possibility of consideration of many k points in the Brillouin zone which are required for describing optical processes (transitions). Besides, the full-potential version describes more efficiently the interstitial-induced properties in low dimension compared to the atomic sphere approximation successfully used in bulk systems. The local spin-density approximation (LSDA) is used with the exchange-correlation functional in the Vosko-Wilk-Nusair parametrization [18] of the Ceperley-Alder results [19] within the spin-density-functional formalism. The basis set consists of Hankel functions for the s , p , and d electrons augmented to numerical solutions of the radial Schrödinger equation at three different energies. In the interstitial region the potential and the charge density are represented by linear combinations of Hankel functions fitted to the values and slopes on the atomic spheres. For the calculation of the nonlinear Kerr spectrum we extract after the self-consistency cycle the eigenvalues and the eigenfunctions at all k -points. We performed calculations of free-standing *bcc* iron films within a slab geometry [20].

This type of *ab initio* calculation permits now to determine the thickness dependence of the nonlinear Kerr spectrum including characteristic features of the electronic and geometric structure of films. It is of interest to compare the *ab initio* calculated results with those obtained from tight-binding calculations to shed more light on approximations. Thus, we present results for the surface of bulk material using the semi-empirical interpolation scheme as in previous studies [6,15]. In addition, we calculate the Kerr spectra of films by simply scaling the d -electron bandwidth of the bulk according to $W \sim \sqrt{Z}A$, where Z refers to an effective coordination number and A is the hopping integral. This simulates the change in the coordination number due to the film dimension. The s -band width is kept unchanged, since mainly d electrons contribute to $\chi^{(2)}$ in the low frequency range. In particular, this is a very rough approximation for MOKE.

Finally, we have performed a direct (unscaled) two-dimensional tight-binding calculation of a monolayer for d electrons only using a quadratic lattice to which *fcc* and *bcc* structures simplify in two dimensions. From these various calculations we will learn about the necessity

to perform *ab initio* calculations rather than tight-binding calculations to determine the characteristic features of the thin-film Kerr spectra.

To shed light on structural film effects, we have performed *ab initio* calculations of nonlinear Kerr spectra for Fe monolayers with different lattice constants.

To check the perturbative treatment of spin-orbit coupling resulting from the wave functions [see Eq. (1)] we have also calculated $\chi^{(2)}$ by including exactly the spin-orbit coupling in the energy eigenvalues. The spin-orbit dependent Hamiltonian is used in the form of Bennett *et al.* [21]. Since in iron the majority and minority pure *d* bands are separated by a large exchange splitting of $J_0=1.78$ eV, the spin-orbit coupling cannot mix the spin up and spin down bands and the only influence of spin-orbit interaction on the energy bands in the Fe *d* bands appears at points of band crossing where the degeneracy of the bands is lifted and the crossing points transform into extrema [22].

III. RESULTS

In Figs. 1 and 2 results are shown for the thickness dependence of the magneto-optical Kerr spectra of *bcc* Fe films obtained from *ab initio* calculations. The film specific features are recognized by comparing the results for the surface of corresponding bulk materials. In Fig. 1(a) the surface sensitivity was simulated by using the factor $1/n^3$. Note, the differences between the nonlinear and linear spectra. In the nonlinear monolayer spectrum the first minimum is shifted compared to the surface of bulk spectrum by about 2 eV to lower energies. This results from the reduced *d*-band width of a film. Furthermore, the tiny maximum at 5.6 eV in the surface of bulk spectrum gets enhanced and shifted to 4.5 eV, having then a width of nearly 3 eV in the case of a monolayer spectrum. In the nonlinear case the position of the minimum between 2 and 4 eV and the slope up to 5.5 eV in the 7 layer spectrum lie close to the surface of bulk spectrum. Note, consistent with our approximation regarding the surface sensitivity, both film results and the surface of bulk spectrum converge. The first minimum around 1 to 2 eV is deepest for a monolayer.

In Fig. 2 the nonlinear spectra were obtained by simulating the surface sensitivity using the approximation (b) $C = W_{\mathbf{k}+2\mathbf{q}_{\parallel},l''\sigma}W_{\mathbf{k}+\mathbf{q}_{\parallel},l'\sigma}W_{\mathbf{k}l\sigma}$, which is the better approximation for the nonlinear case. Consistent with this approximation the structure changes not too

much going from three to five to seven monolayers. Thus, the essential contribution to NOLIMOKE results from the surface layer, however, the electronic structure of this layer is affected by the other layers due to hybridization and next-nearest neighbor interaction. This point is corroborated by the results for the monolayer. The results are different from those for the surface of bulk spectrum, where we have used the truncated bulk approximation. One should also note the layer dependent change of the depth of the first minimum which is related to the value of the magnetization in the top layer.

In Fig. 1(b) we also present results for the linear Kerr effect in order to compare with the nonlinear case and with recent experiments. The amplitudes in the linear spectrum are scaled with the film thickness, e.g. by $1/n^2$. Without such scaling the spectra will grow with increasing film thickness. Note, the film and surface of bulk spectra converge as it should be. The linear spectra of the 7 layer film and of the truncated bulk do not differ up to 5 eV. In the linear monolayer spectrum the transitions between majority spin electron bands begin to dominate at energies higher 3.3 eV (sign change). In the optical range we find a new structure at 5.2 eV.

In agreement with experiment [8,9] we observe the shift of the first peak with respect to the one and three monolayer spectra. It is interesting that we do not obtain the extra peak in the linear spectrum of thin films. This supports the interpretation of this peak as resulting of quantum-well-state transitions.

In Fig. 3 we show results for the nonlinear magneto-optical Kerr spectra for a Fe monolayer assuming different lattice constants to simulate film-structure effects. We compare spectra obtained using the Fe bulk lattice constant $a=2.76 \text{ \AA}$ (determined by total energy minimization), using $a=2.776 \text{ \AA}$ corresponding to a Fe monolayer on Au, and $a=2.783 \text{ \AA}$ corresponding to Fe on Ag, and using the experimental Fe lattice constant $a=2.88 \text{ \AA}$. The values for Au and Ag follow from the theoretical lattice constant applying the experimental lattice mismatch. Whereas the amplitude of the general minimum at about 1.5 eV shows no clear dependence on the lattice constant, the energy for which $Im\chi^{(2)}$ changes sign corresponds quantitatively to the ratios of the lattice constants. Thus, we demonstrate that NOLIMOKE reflects sensitively structural changes.

To gain more information about the possibility of using tight-binding methods for treat-

ing thin films we compare with *ab initio* results in Fig. 4. First, note that the *ab initio* and the semi-empirical tight-binding spectra of the bulk surface agree rather well in the optical range. However, the calculations for the monolayer using *ab initio* or different tight-binding methods differ drastically. Curve 5 is obtained by including in the hopping parameters correlations effects and the reduced number of nearest neighbors of a monolayer. The situation is similar in the linear case, see Fig. 4(b).

This comparison illustrates that bulk tight-binding parameters are acceptable for the Kerr spectra at the bulk surface but not at films. Here, a tight-binding method may be successful using specific parameters for every film layer. If appropriate film parameters are unavailable *ab initio* calculations are mandatory to obtain the specific film features.

In Fig. 5 we demonstrate the effects resulting from including non-perturbatively the spin-orbit coupling also in the electronic energies $E_{\mathbf{k}\ell\sigma}$. Since in the case of Fe spin-orbit coupling does not mix the minority and majority spin bands we find a negligible effect.

IV. DISCUSSION

We learn from our results obtained by an electronic theory that NOLIMOKE reflects sensitively the electronic structure of thin films. In contrast to the MOKE signal the NOLIMOKE signal originates for flat surfaces essentially from the surface layer [23]. However, the electronic structure of this layer depends on the film thickness. This can be clearly seen in our results. Very interesting are also the results for Fe on a Ag and Au substrate, simulated by the lattice constant of the Fe monolayer, since they demonstrate that even structural effects are reflected in the NOLIMOKE spectra. This is of general interest regarding film growth and structural changes occurring as a function of film thickness.

We emphasize that characteristic features of magnetism in thin films like changes of the magnitude of the magnetic moments and of the magnetization can be seen in the NOLIMOKE spectra. Particularly, this can be seen from the depth of the minimum in $\chi^{(2)}$ around 3 eV. The enhanced minimum results from an increase of the magnetic moments. Actually, we obtain an enhanced moment of $2.8 \mu_B$ in the first film layer. Since the magnitude of the magnetic moment is a fingerprint of the geometric structure this can be used to determine the film geometry. While MOKE already reflects characteristic film-averaged features,

NOLIMOKE clearly exhibits further interesting details. Both MOKE and NOLIMOKE are suitable to study thin films in a material-specific way, however only NOLIMOKE can be used to study interface effects for which we expect similar features as for the surface. Our results (see Figs. 5a and 5b) support once again that it is sufficient for transition metals to treat spin-orbit coupling by non-degenerate linear perturbation theory applied to the wave functions. This is physically expected [15].

The comparison of the *ab initio* results with semi-empirical tight-binding calculations shows that it is necessary to use *ab initio* calculations for the films if only bulk tight-binding parameters are available. However, tight-binding calculations may be adequate if one uses as input parameters those determined from *ab initio* calculations for thin films.

Concerning comparison with experiment it has been observed in agreement with our theory that the MOKE signal increases linear with the film thickness up to 20 monolayers whereas the NOLIMOKE signal remains nearly constant. Our theory suggests that the experimental enhancement of the NOLIMOKE signal for 3 and 4 layer films at a frequency of 1.55 eV (corresponding to a wavelength of 800 nm, see Fig. 5 in [12]) results from the electronic structure and in particular from the enhancement of the surface magnetization. Furthermore, the experiments describing the thickness dependence of the MOKE or NOLIMOKE signals are usually performed at one fixed frequency. Our calculations have shown that for very thin films structures of the Kerr spectra are shifted due to changes in the electronic structure of the films. Thus, the Kerr susceptibility at a fixed frequency does not show a monotonous increase with increasing film thickness depending on the choice of the frequency respective to the spectrum structure.

The onset of the NOLIMOKE signal due to the appearance of magnetism will reflect the structure of the surface. For flat surfaces, the slope of the signal should be much larger than for corrugated surfaces. For film thickness larger than a few atomic layers the NOLIMOKE signal will remain nearly constant, while the MOKE signal increases with film thickness. An enhanced magnetization in thin films is reflected by an enhanced NOLIMOKE signal.

Regarding the enhancement of magnetic moments in thin films we deduce from our NOLIMOKE spectra for a three layer thick film $\mu_{surface} = 2.64 \mu_B$. From our electronic bandstructure we obtain directly a film averaged magnetic moment of $2.62 \mu_B$. From po-

larized neutron reflection for a 5.5 monolayer Fe film on Ag(001) covered by Ag Bland *et al.* [24] deduced an averaged magnetic moment of $2.58 \mu_B$. Here again the comparison of MOKE and NOLIMOKE spectra can clear up whether the magnetic moments are enhanced (at the film-substrate interface or at the film-vacuum interface, or at both).

Since we present also the first theoretical results of the thickness dependence of the linear magneto-optical Kerr spectra we compare these with recent experiments by Suzuki *et al.* [8] and Geerts *et al.* [9]. In agreement with these experimental results we obtain the shift of the first minimum in $\chi^{(1)}$ dependent on the film thickness and a quick convergence towards bulk results for more than four layers. Note, we have not included the confinement of the substrate electrons and thus quantum-well-states effects are not included in the calculation.

For future studies on NOLIMOKE it will be interesting to extend calculations to multilayer systems and to analyze in more detail interface contributions and lateral resolution. A first principle evaluation of SHG should show that essentially only surface and interface layers contribute and that second layer contributions are of less importance, since the breakdown of inversion symmetry is not as strongly felt as in the interface layer. Furthermore, it is possible to extract the magnetic easy axis at interfaces from NOLIMOKE [25]. In particular, we will extend our NOLIMOKE calculations to analyze *bcc* vs. *fcc* Fe structure on a substrate during film growth.

REFERENCES

- ¹ U. Pustogowa, W. Hübner, and K. H. Bennemann, Phys. Rev. B **49**, 10031 (1994); Appl. Phys. A **59**, 611 (1994).
- ² J. Reif, J. C. Zink, C.-M. Schneider, and J. Kirschner, Phys. Rev. Lett. **67**, 2878 (1991).
- ³ J. Reif, C. Rau, and E. Matthias, Phys. Rev. Lett. **71**, 1931 (1993).
- ⁴ Bert Koopmans and Theo Rasing, to be published.
- ⁵ K. Böhmer, J. Hohlfeld, and E. Matthias, Appl. Phys. A **60**, 203 (1995).
- ⁶ U. Pustogowa, W. Hübner, and K. H. Bennemann, Phys. Rev. B **48**, 8607 (1993).
- ⁷ H. A. Wierenga, M. W. J. Prins, D. L. Abraham, and Th. Rasing, Phys. Rev. B **50**, 1282 (1994).
- ⁸ Yoshishige Suzuki, Tashikazu Katayama, Sadafumi Yoshida, and Kazunobu Tanaka, Phys. Rev. Lett. **68**, 3355 (1992).
- ⁹ Wim Geerts, Y. Suzuki, T. Katayama, K. Tanaka, K. Ando, and S. Yoshida, Phys. Rev. B **50**, 12581 (1994).
- ¹⁰ J. Thomassen, F. May, B. Feldmann, M. Wuttig, and H. Ibach, Phys. Rev. Lett. **69**, 3831 (1992).
- ¹¹ Dongqi Li, M. Freitag, J. Pearson, Z. Q. Qui, and S. D. Bader, Phys. Rev. Lett. **72**, 3112 (1994).
- ¹² T. Rasing, Appl. Phys. A **59**, 531 (1994).
- ¹³ H. A. Wierenga, W. de Jong, M. W. J. Prins, Th. Rasing, R. Vollmer, A. Kirilyuk, H. Schwalbe, and J. Kirschner, Phys. Rev. Lett. **74**, 1462 (1995).
- ¹⁴ W. Hübner and K. H. Bennemann, Phys. Rev. B **40**, 5973 (1989).
- ¹⁵ W. Hübner, Phys. Rev. B **42**, 11553 (1990).
- ¹⁶ M. Methfessel, Phys. Rev. B **38**, 1537 (1988); M. Methfessel, C. O. Rodriguez, and O.

- K. Andersen, *ibid.* **40**, 2009 (1989); M. Methfessel and M. Scheffler, *Physica B* **172**, 175 (1991).
- ¹⁷ T. Kraft, P. M. Marcus, and M. Scheffler, *Phys. Rev. B* **49**, 11511 (1994).
- ¹⁸ S. H. Vosko, L. Wilk, and M. Nusair, *Can. J. Phys.* **58**, 1200 (1980).
- ¹⁹ D. M. Ceperley and B. J. Alder, *Phys. Rev. Lett.* **45**, 566 (1980).
- ²⁰ U. Pustogowa, W. Hübner, K. H. Bennemann, in print *J. Mag. Mag. Mater.* (1995).
- ²¹ A. J. Bennett und B. R. Cooper, *Phys. Rev. B* **3**, 1642 (1971).
- ²² T. Moos, W. Hübner, and K. H. Bennemann, submitted for publication.
- ²³ This can also be seen from first principle calculations treating properly the matrix elements in $\chi^{(2)}$ which sense the breakdown of inversion symmetry which is necessary for a SH signal. Such calculations are in progress; U. Pustogowa *et al.*, to be published.
- ²⁴ J. A. C. Bland, C. Daboo, B. Heinrich, Z. Celinski, and R. D. Bateson, *Phys. Rev. B* **51**, 258 (1995).
- ²⁵ W. Hübner and K. H. Bennemann, submitted for publication.

FIGURES

FIG. 1. *Ab initio* calculated (a) nonlinear and (b) linear magneto-optical Kerr spectra of Fe for a truncated bulk surface (solid line), a monolayer (dashed curve), films having 3 layers (dashed-dotted), 5 layers (long-dashed), and 7 atomic layers (dotted curve). The second harmonic response of the surface layer results by averaging the electronic input structure over the whole film.

FIG. 2. *Ab initio* calculated nonlinear magneto-optical Kerr spectra of Fe for a truncated bulk surface (solid line), a monolayer (dashed curve), 3 layers film (dashed-dotted), 5 layers (long-dashed), and 7 atomic layers (dotted curve). The second harmonic response results from the first atomic layer. This SH response is obtained by projecting the wave functions to the first atomic layer yielding the factor C .

FIG. 3. Film-lattice-constant dependence of *ab initio* calculated nonlinear Kerr spectra of a Fe monolayer. The solid curve refers to the bulk *bcc* Fe lattice constant, the dashed curve to $a=2.776$ Å(bulk Au), and the dotted curve to $a=2.783$ Å(bulk Ag). The long-dashed curve refers to the experimental a for Fe. The inset shows at an enhanced scale the effects of different lattice constants for the zero of $\text{Im } \chi^{(2)}$ at $\hbar\omega \approx 3$ eV.

FIG. 4. Comparison of *ab initio* and semi-empirical calculations of the (a) nonlinear and (b) linear magneto-optical susceptibilities of Fe. The bulk surface results from truncating bulk and the semi-empirical calculations for a monolayer are performed with reduced hopping parameters A_0 .

FIG. 5. Role of spin-orbit coupling: Semiempirically calculated (a) nonlinear and (b) linear magneto-optical Kerr spectra of a Fe monolayer with spin-orbit coupling in first order perturbation theory (dotted curve) and treated non-perturbatively (dashed curve). Δ gives the difference.

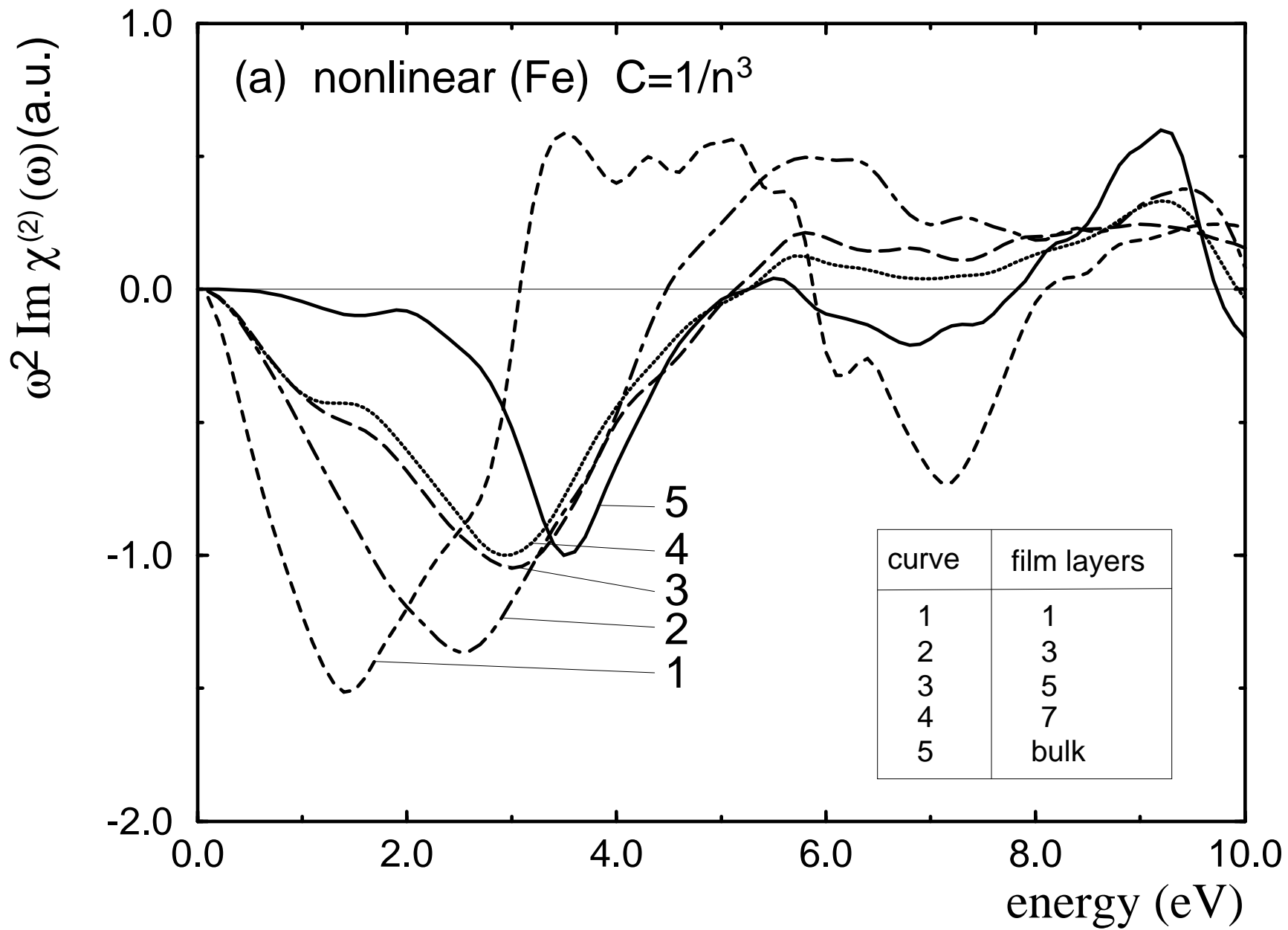


Fig. 1(a)

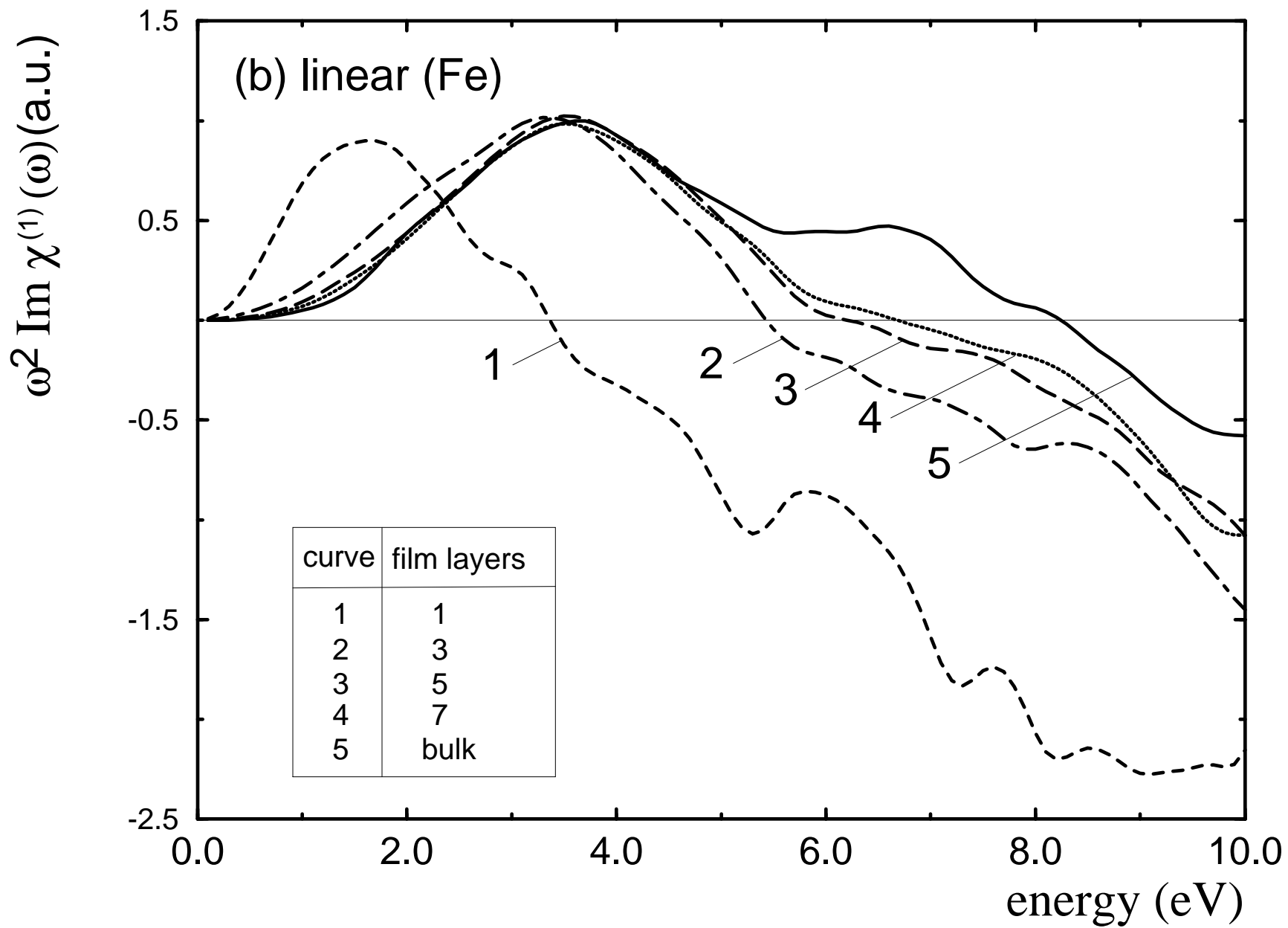


Fig. 1(b)

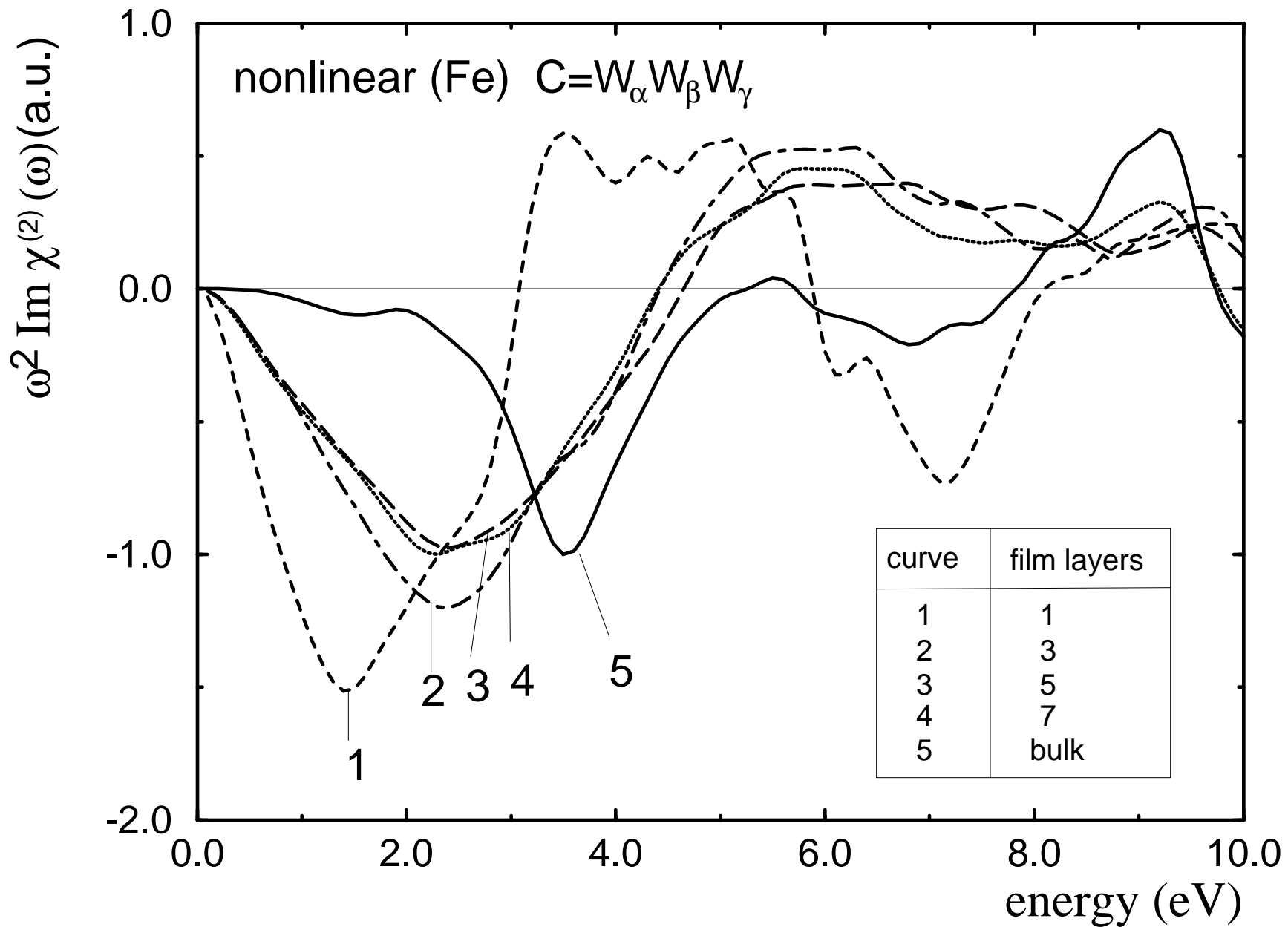


Fig. 2

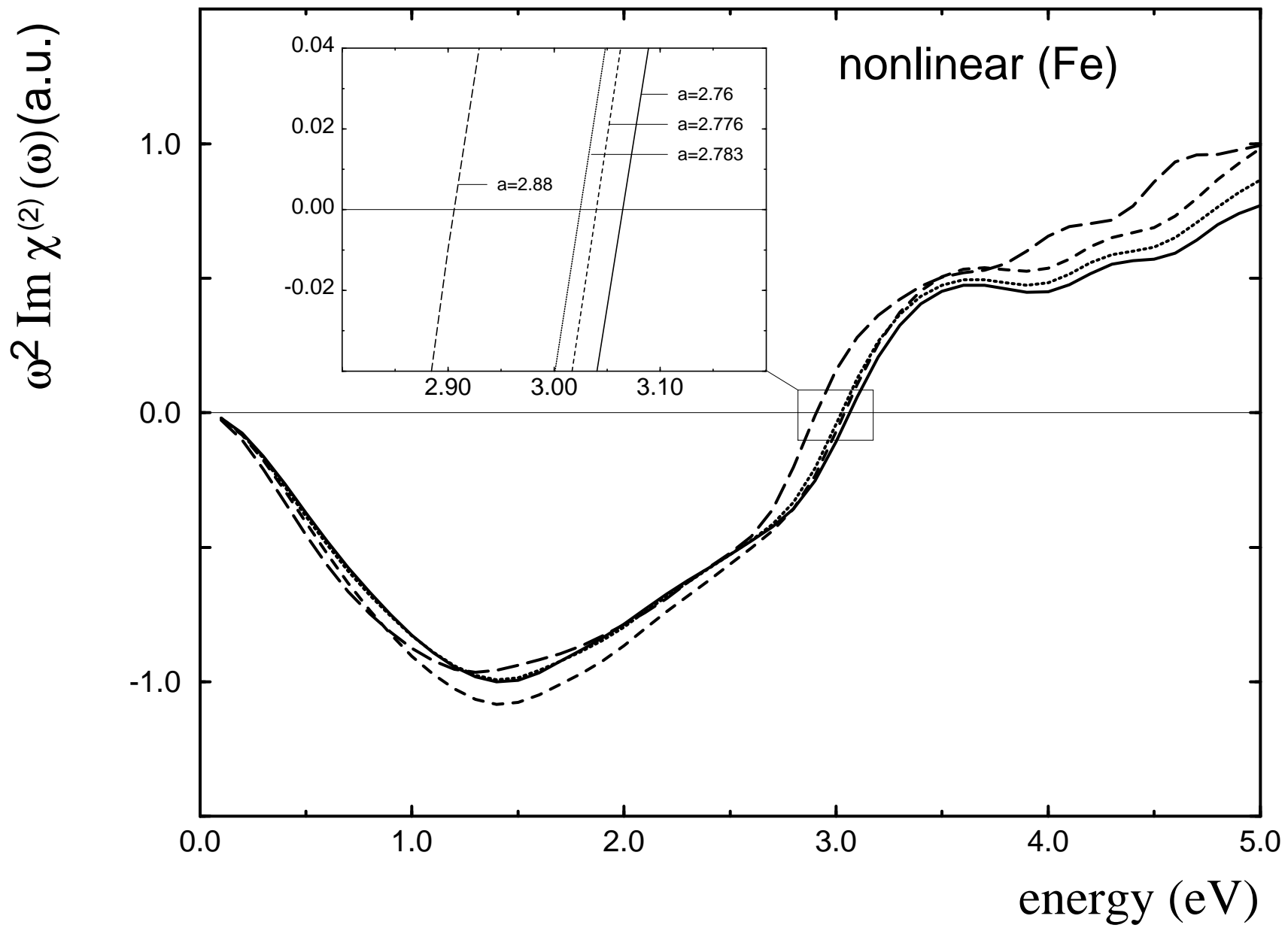


Fig. 3

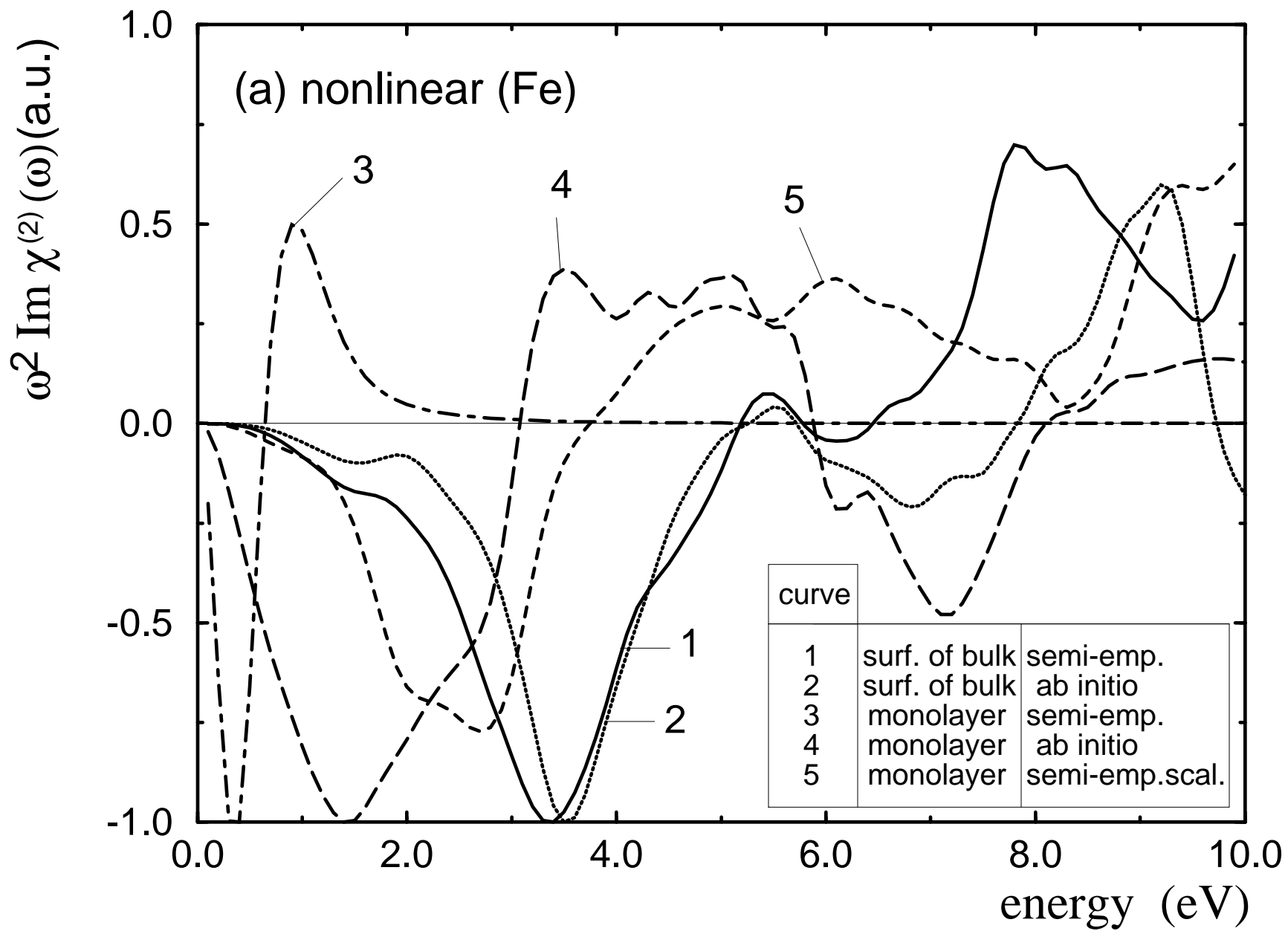


Fig. 4(a)

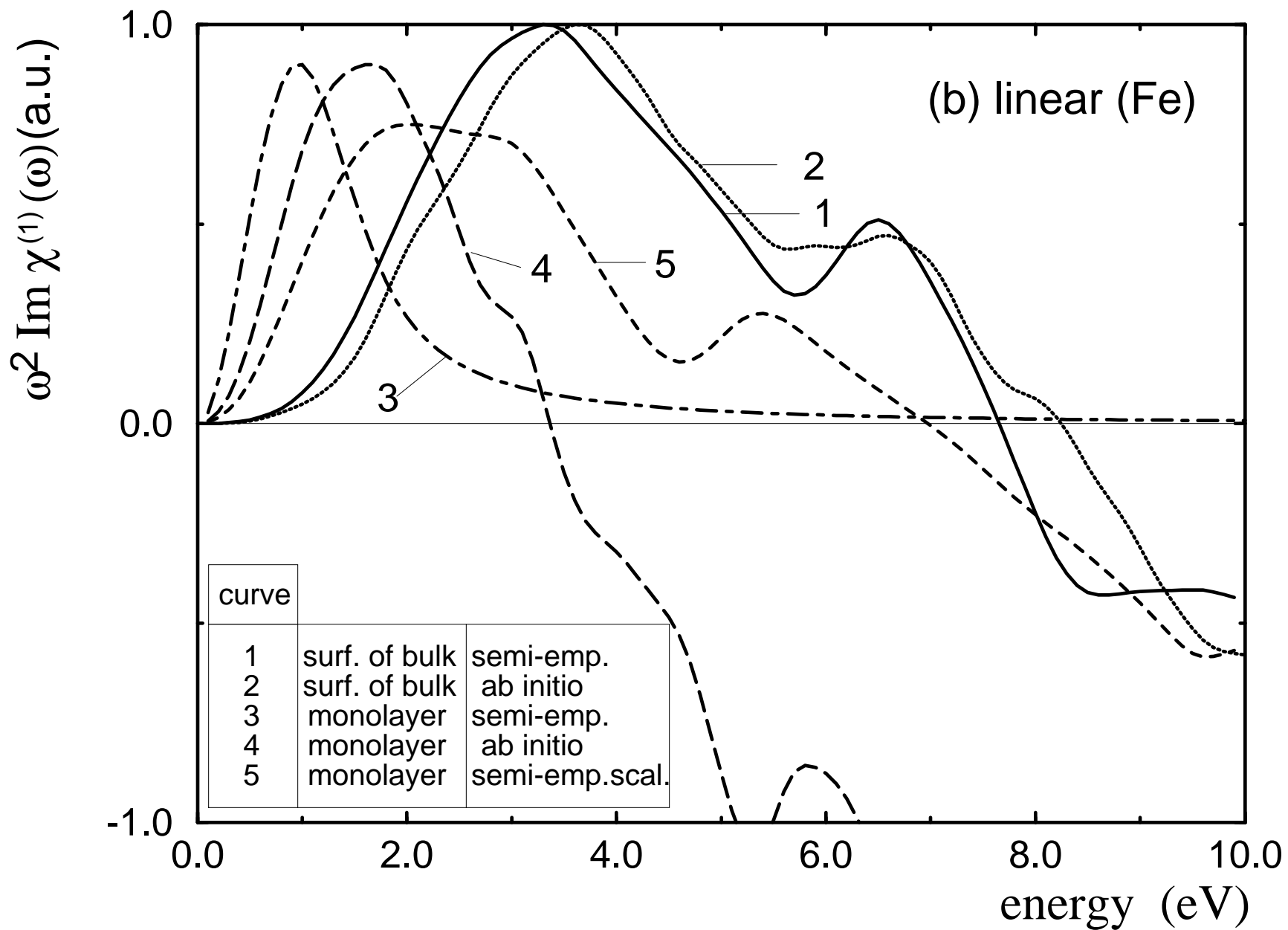


Fig. 4(b)

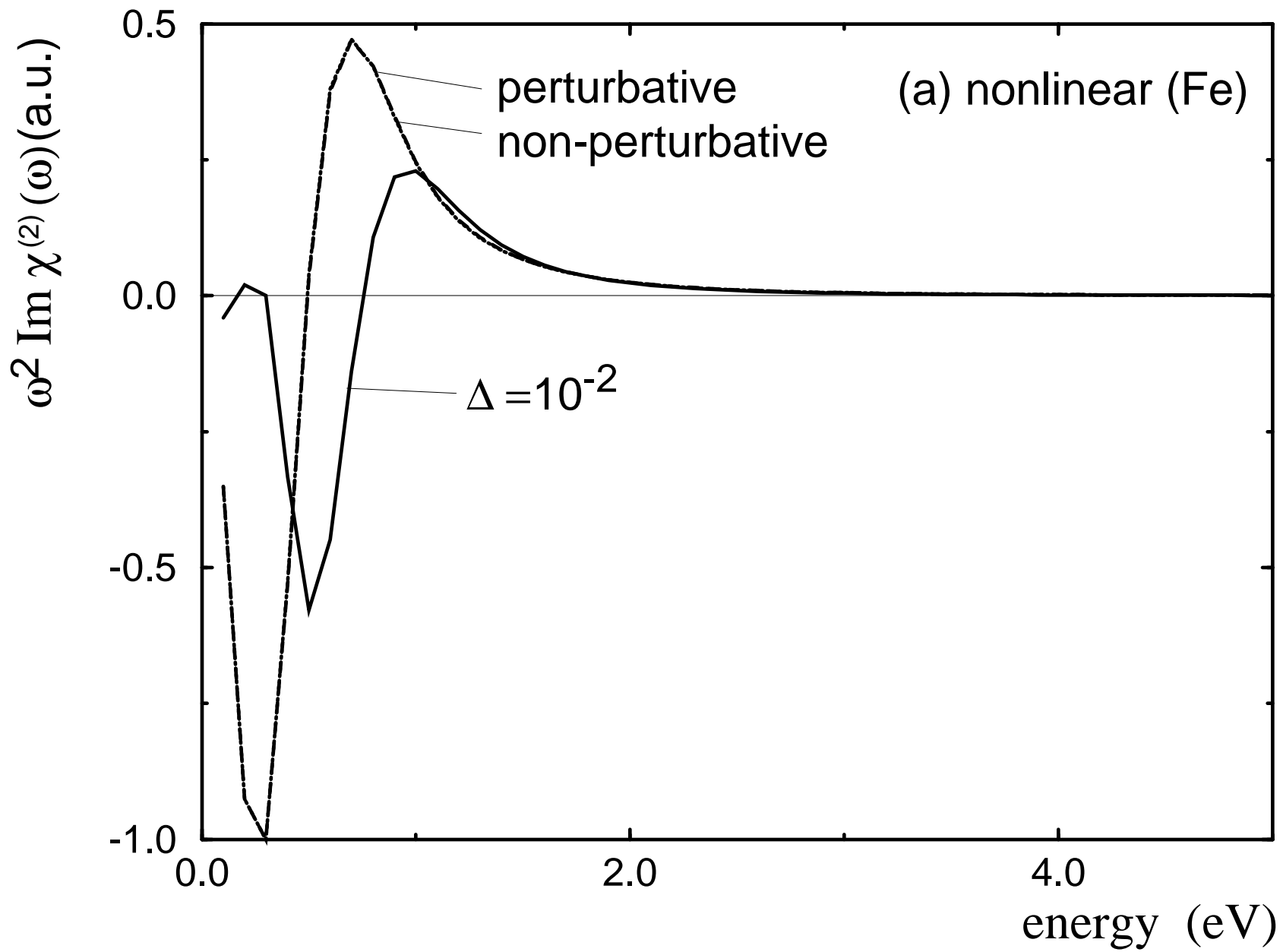


Fig. 5(a)

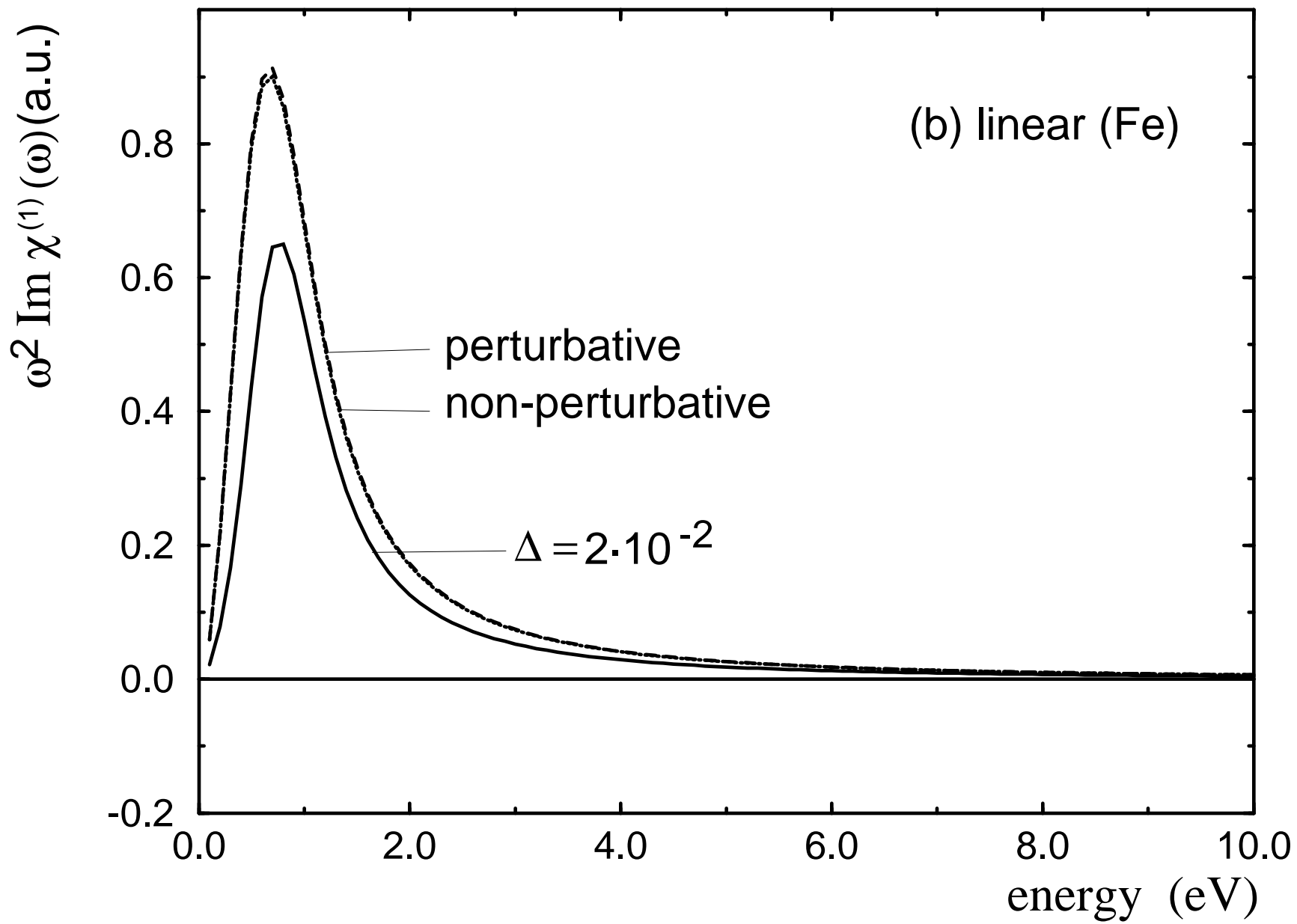


Fig. 5(b)